

Automated Comet Assay Imaging and Dual-Mask Analysis to Determine DNA Damage on an Individual Comet Basis

Authors

Brad Larson
Agilent Technologies, Inc.

Asha Sinha and Sachin Katyal,
University of Manitoba

Introduction

Mammalian cells incur DNA damage and alterations as a result of internal factors, such as stress, environment, oxidation and metabolism, as well as exposure to external stimuli, such as chemical compounds, UV and cosmic radiation. Genotoxicity studies aim to identify and understand the mechanisms of DNA damage and repair, and also to seek methods of pathway regulation and dysregulation for improved therapeutic success. Beyond therapeutic implications, a number of industries, including cosmetics, food and beverage, chemical, and mining/oil/petroleum incorporate genotoxicity testing to characterize the safety profile of their products.

The comet assay, or single cell gel electrophoresis (SCGE), is well established as a direct measure of DNA damage in genotoxicity studies. Typically, neutral comet is used to detect DNA double-stranded breaks while alkali comet detects a wider breadth of DNA lesions including DNA single-stranded breaks and abasic sites. Using this method, cells exposed to a test compound are embedded in agarose, lysed to remove membranes and histones, treated with an alkali solution to unwind and denature the DNA (in the case of alkali comet), and subjected to an electric field to separate DNA fragments from intact DNA molecules based on differences in charge to mass ratio. Upon fluorescent staining and imaging, the result appears similar to a comet, where DNA fragments (comet tail) migrate through the gel matrix while intact/undamaged DNA remains static (comet head). Commonly generated metrics such as percentage of fragmented DNA in the comet tail and tail moment are a direct measure of cellular DNA damage following treatment.

Fluorescence microscopy is the standard method for measuring these parameters. Typically, detection requires operator intervention for image capture and analysis which tends to be a slow process, limiting sample throughput. Furthermore, operator subjectivity during analysis can also skew results as only comets that meet personal criteria are chosen for inclusion in the data set. Incorporating automated image acquisition and analysis into the assay workflow can help to enhance sample throughput, assay robustness and accuracy, while also increasing the overall laboratory efficiency.

The ability to generate data on a per-comet basis is also preferable when measuring the effect of a potential damaging or healing agent. While average percent DNA in the comet tail and tail moment data allows for assessment of a population captured within an image or set of images, it does not allow for the most efficient scrutiny of individual comets to ascertain why damage was seen at a particular level within the imaged sample set. Incorporating methods to calculate results from multiple areas linked to a particular comet provides population and individual comet data, providing a more complete data set.

This application note demonstrates a method to automate detection and analysis of high throughput comet-based genotoxicity data. Using a novel cell imaging multimode reader and high-density slides, 96 individual samples may be processed and analyzed simultaneously. Advanced analysis software with dual-mask capability links comet head and tail information per comet so that real-time population-level data, as well as individual comet data, are available for use in percent DNA in the tail and comet tail moment calculations.

Materials and methods

Materials

Cells

U251 (human glioma) cells (part number 09063001) were purchased from Sigma-Aldrich (Saint Louis, MO).

Assay and experimental components

LM Agarose (part number 4250-050-02), 96-well CometSlides (part number 4253-096-03), lysis buffer (part number 4250-050-01) and CometAssay electrophoresis system (part number 4250-050-ES) were obtained from Trevigen, Inc. (Gaithersburg, MD). SYBR Gold nucleic acid gel stain (part number S-11494, ThermoFisher, Carlsbad, CA), diluted to 1x, was also supplied by Trevigen, Inc. The known topoisomerase-1 inhibitor (cytotoxin), camptothecin (part number 208925) was purchased from EMD Millipore (Billerica, MA).

Agilent BioTek Cytation 5 cell imaging multimode reader

Agilent BioTek Cytation 5 is a modular multimode microplate reader combined with automated digital microscopy. Filter- and monochromator-based microplate reading are available, along with laser-based excitation for alpha assays. The microscopy module provides up to 60x magnification in fluorescence, brightfield, color brightfield and phase contrast. With special emphasis on live-cell assays, Cytation 5 features shaking, temperature control to 65 °C, CO₂/O₂ gas control and dual injectors for kinetic assays. The instrument was used to image the stained DNA using the GFP imaging channel. Integrated Agilent BioTek Gen5 microplate reader and imager software controls Cytation 5, and also automates image capture, analysis and processing. A two-part adapter (part number 1322144) was used when imaging the 96-well CometSlide to ensure consistent positioning.

Methods

Standard alkaline comet assay performance

Cultured U251 cells were treated with concentrations of camptothecin ranging from 0 to 10 µM, embedded in 1% low melting agarose, and immobilized on a specially treated 96-well slide to promote adherence. The slide was then immersed in lysis buffer for 30 to 60 minutes at 4 °C to remove membranes and histones from the DNA, followed by a 30-minute room temperature equilibration in pH 13 alkaline electrophoresis buffer to unwind and denature the DNA. Alkaline electrophoresis was performed for 30 to 45 minutes at 4 °C and 1 V/cm using the CometAssay electrophoresis system. Slides were neutralized and agarose dried down before staining the DNA with SYBR Gold. Stained slides were then imaged by the Cytation 5 using the parameters listed in Table 1.

Table 1. Automated comet imaging parameters.

Imaging Parameters	
First Imaging Channel	GFP
Second Imaging Channel	GFP
Objective	Meiji 2.5x
Montage	2 Rows by 1 column
Montage Overlap	Auto for stitching
Exposure	Auto exposure based upon positive and negative control wells

Gen5 dual mask comet analysis

Primary mask cellular analysis criteria (Table 2) were applied to automatically place object masks around comet heads in each captured image. Auto threshold was selected and the slider bar moved to a value of -35. Secondary mask cellular analysis criteria (Table 3) were then also applied to place a linked additional mask around the entire comet.

Table 2. Comet head analysis parameters.

Primary Cellular Analysis Parameters	
Threshold	Auto (-35)
Background	Dark
Split Touching Objects	Checked
Fill Holes in Masks	Checked
Min. Object Size	45 µm
Max. Object Size	100 µm
Include Primary Edge Objects	Unchecked
Analyze Entire Image	Checked
Advanced Detection Options	
Background Flattening Size	50 µm (rolling ball diameter)
Image Smoothing Strength	3 Cycles of 3 × 3 average filter
Evaluate Background On	5% of lowest pixels
Primary Mask	Expand the threshold mask 10 µm

Table 3. Total comet analysis parameters.

Secondary Cellular Analysis Parameters	
Measure Within a Secondary Mask	Include primary and secondary area in analysis
Expand Primary Mask	120 µm
Threshold	5,000
Background	Dark
Method	Propagate mask

Results and discussion

Automated 96-well comet imaging and preprocessing

U251 cells were exposed to various concentrations of camptothecin and processed using the 96-well CometSlide format. Agilent BioTek Cytation 5 automatically imaged the CometSlide using previously determined well locations in the plate layout for the incorporated slide, thus eliminating manual determination of comet locations. Exposure parameters were set such that fluorescence values per pixel were within the CCD camera’s quantifiable range, while autofocus and image montage creation were also performed.

Following image capture, multiple steps were automatically carried out in Gen5 software to properly prepare each image for analysis. These steps improve robustness of

the generated data from each test sample. The first step processed the image to remove background signal using the criteria in Table 4. The rolling ball diameter value of 1,500 µm was chosen to ensure that adequate areas of the image were included in the determination of background signal from true comet signal. As the signal from the tail portion of the comet can be relatively weak, depending on the level of DNA damage, analysis of smaller portions of the image to determine background signal can skew results, causing signal from the comet tails to be falsely removed. Incorporation of the larger diameter creates preprocessed images with a reduced background, for more accurate identification of the fluorescent signal from actual comets without affecting final results.

Table 4. Image preprocessing parameters.

Image Preprocessing Parameters	
Background	Dark
Rolling Ball Diameter	1,500 µm
Image Smoothing Strength	0
Second Image Parameters	Same as first image

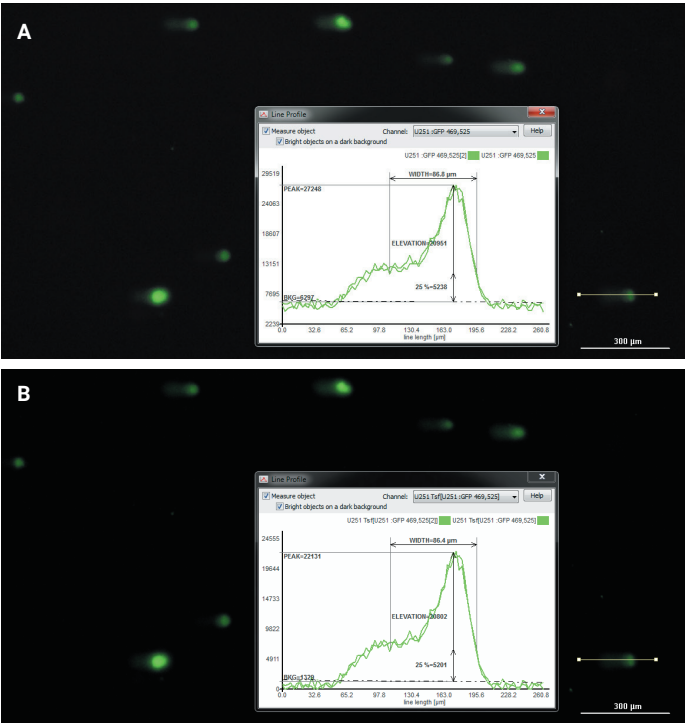


Figure 1. Image background signal removal via preprocessing. Zoomed 2.5x images (A) before; (B) or after Table 4 preprocessing criteria applied using Agilent BioTek Gen5 software. Inset graphs in (A) and (B) represent a cross-section of green fluorescence intensity across a single comet obtained using the Gen5 line analysis tool. The individual comet measured is visible immediately to the right of the inset graph. The length of the line used is represented by the X-axis of the inset graph.

In the second step, Gen5 automatically stitched together the two individually captured images in their original configuration so that comet placement in the final combined image was identical to that seen in the well.

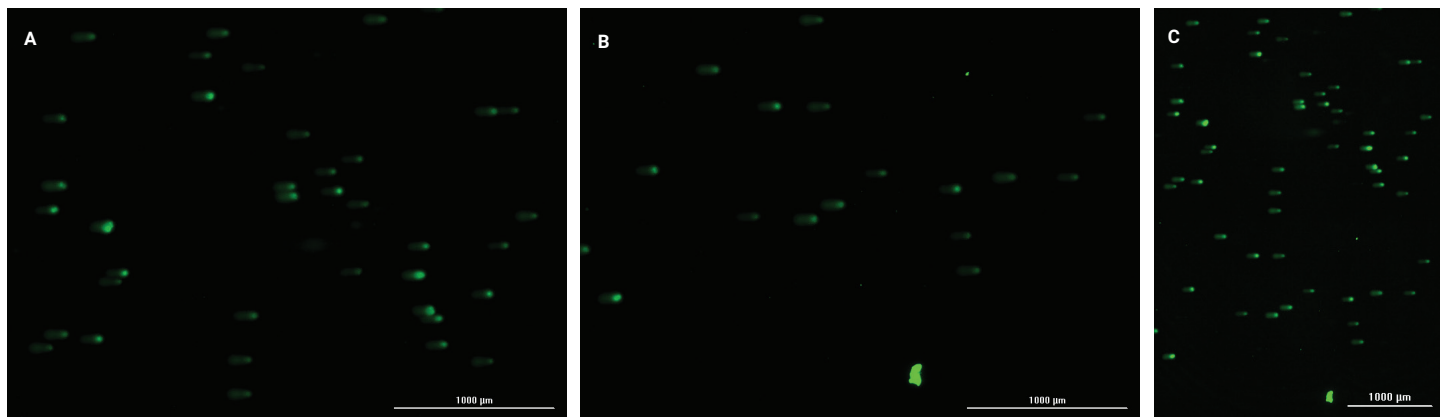


Figure 2. Image stitching. 2.5x images of (A and B) individual image montage tiles; and (C) final stitched image using Agilent BioTek Gen5 software.

The final images accurately portrayed the extent of DNA damage from each test condition, where untreated comets (Figure 3A) appeared as well-defined spheres, or comet heads, while those treated with camptothecin showed progressive DNA damage in the form of a distinct comet tail (Figures 3B and 3C).

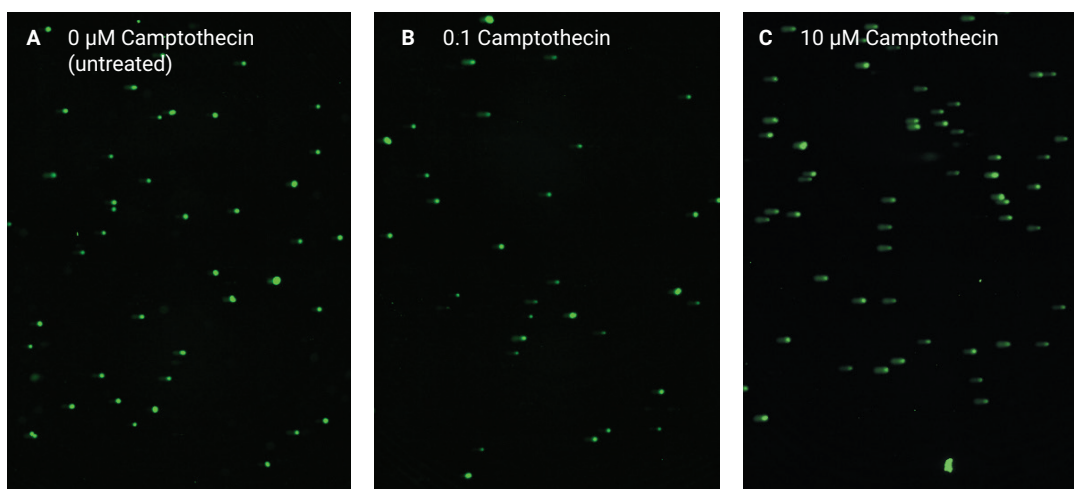


Figure 3. Automated comet analyses based on user-programmed cellular analysis parameters. Images captured using a 2.5x objective, 1 × 2 montage images of stained comets from single well using U251 cells exposed to (A) 0 µM (untreated) camptothecin; (B) 0.1 µM camptothecin; (C) 10 µM camptothecin, using GFP imaging channel with fluorescent background removed.

Automated dual-mask comet analysis

Primary and secondary cellular analysis criteria (Tables 2 and 3) were applied to all images captured using Cytation 5's integrated Gen5 microplate reader and imager software. Primary cellular analysis automatically masked each comet head (Figure 4A), while secondary analysis automatically masked each comet tail (Figure 4B).

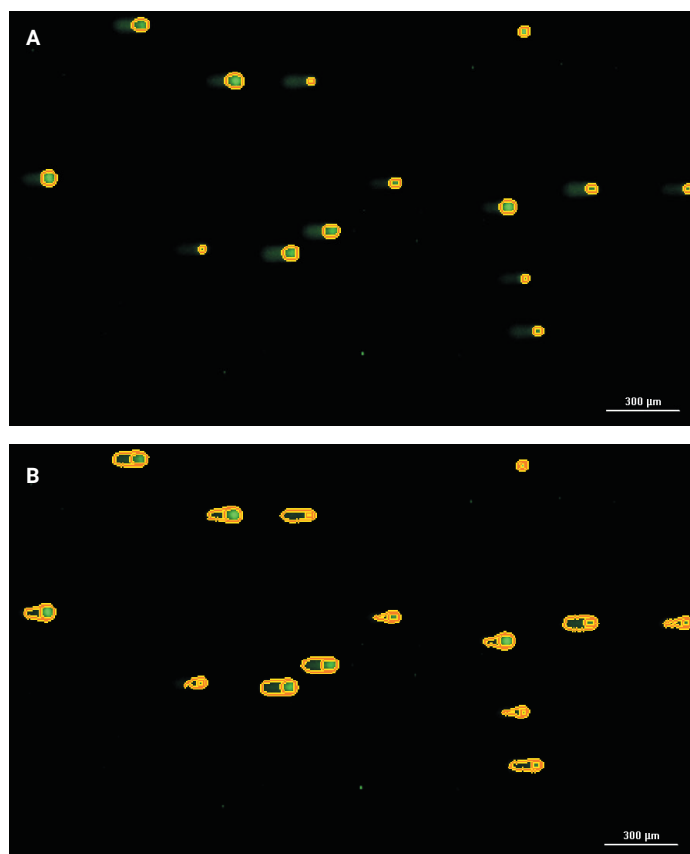


Figure 4. Automated 10 µM camptothecin treated comet analyses based on user-programmed cellular analysis parameters. Primary and secondary cellular analysis object masks showing (A) comet head and (B) comet tail in relation to the comet head, respectively. Images captured using a 2.5x objective, 1 × 2 image montage, and GFP imaging channel.

By using primary cellular analysis to mask the comet heads first, then a secondary mask for the comet tails, each individual comet was properly linked; reducing the occurrence of false results. Further subpopulation analysis may be applied to eliminate overlapping comets, anomalies and other false objects that might be overlooked via subjective methods. The final set of included objects yielded results with a high degree of accuracy and consistency, and allowed population level as well as individual single comet analysis.

Individual comet metric calculations

Once the comet assay procedure and image preparation were complete, multiple calculations were immediately performed using Gen5 microplate reader and imager software, including commonly used assay metrics on an individual comet basis. The first metric was percent DNA in the tail. This value takes into account the total fluorescence within the comet head, containing undamaged DNA; and the comet tail, containing damaged DNA fragments (Figure 5). As explained above, DNA fragments, having a smaller size than intact DNA strands migrate faster through the gel matrix. When fluorescently stained and analyzed as one object, fluorescence increases outside the comet head as a function of the extent of the comet tail; and by proxy, the level of DNA damage.

Gen5 microplate reader and imager software used the following formula and object metrics of interest (Table 5) to automatically calculate the percent DNA in the tail:

$$(1 - (M_1/M_2)) \times 100$$

Table 5. Percent DNA in the tail formula metrics.

Primary Mask		
Calculated Metric	Description	Data Reduction Designation
Integral [GFP]	Integrated GFP fluorescence within the primary mask (comet head)	M ₁
Secondary Mask		
Integral_2[GFP]	Integrated GFP fluorescence within the secondary mask (total comet)	M ₂

When the fraction of comet head fluorescence, in terms of the total comet fluorescent signal, is subtracted from one, the fraction in the comet tail remains. When multiplied by 100, this value then represents the percent DNA in the comet tail.

The second metric was the comet tail moment. Here, the percent DNA in the tail value previously calculated is combined with size measurements of the comet head and tail (Figure 5). With the integration of length measurements, not only is the total amount of damaged DNA taken into account, but also the extent of DNA strand damage. For the greater the number of times a strand is cut, the smaller the created fragments. And by proxy, the smaller the fragment the further the migration through the gel matrix, creating a longer comet tail and a larger tail moment.

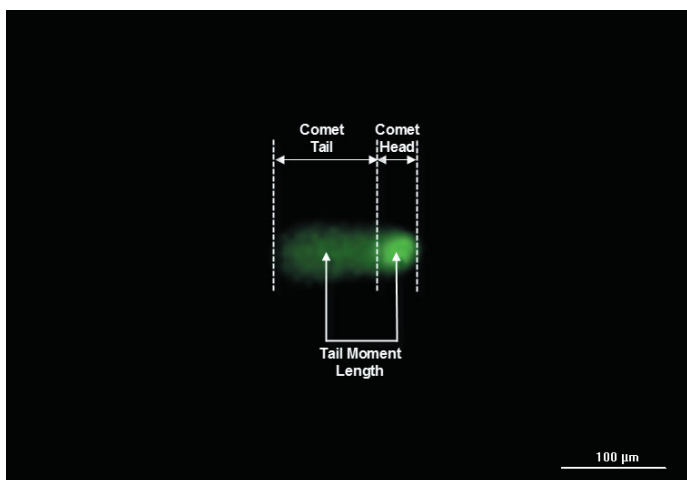


Figure 5. Comet areas included in tail moment calculation.

Gen5 microplate reader and imager software used the following formula and object metrics of interest (Table 6) to calculate the tail moment value:

$$\{[(1 - (M_1/M_2)) \times 100] \times [(M_3/M_5)/2 + (((M_4 - M_3)/M_5)/2)]\}/100$$

Table 6. Comet tail moment formula metrics.

Calculated Metric	Description	Data Reduction Designation
Primary Mask		
Integral [GFP]	Integrated GFP fluorescence within the primary mask (comet head)	M ₁
Area	Area of the primary mask (comet head)	M ₃
Size	Size of the primary mask (comet head)	M ₅
Secondary Mask		
Integral_2[GFP]	Integrated GFP fluorescence within the secondary mask (total comet)	M ₂
Area_2	Area of the secondary mask (total comet)	M ₄

The first portion of the formula calculates the aforementioned percent DNA in the comet tail. The second part of the formula calculates one half the length of the comet head, and the final portion of the formula calculates one half the length of the comet tail. By dividing each area by the comet head size, length values may be used in the final complete formula. As DNA damage increases, the length of the comet tail and percent DNA in the tail also increase, thereby creating a direct correlation between all three phenomena.

By including each formula into the calculated metrics for the cellular analysis step, percent DNA in the comet tail and tail moment may be determined for each comet included in every image taken (Figure 6).

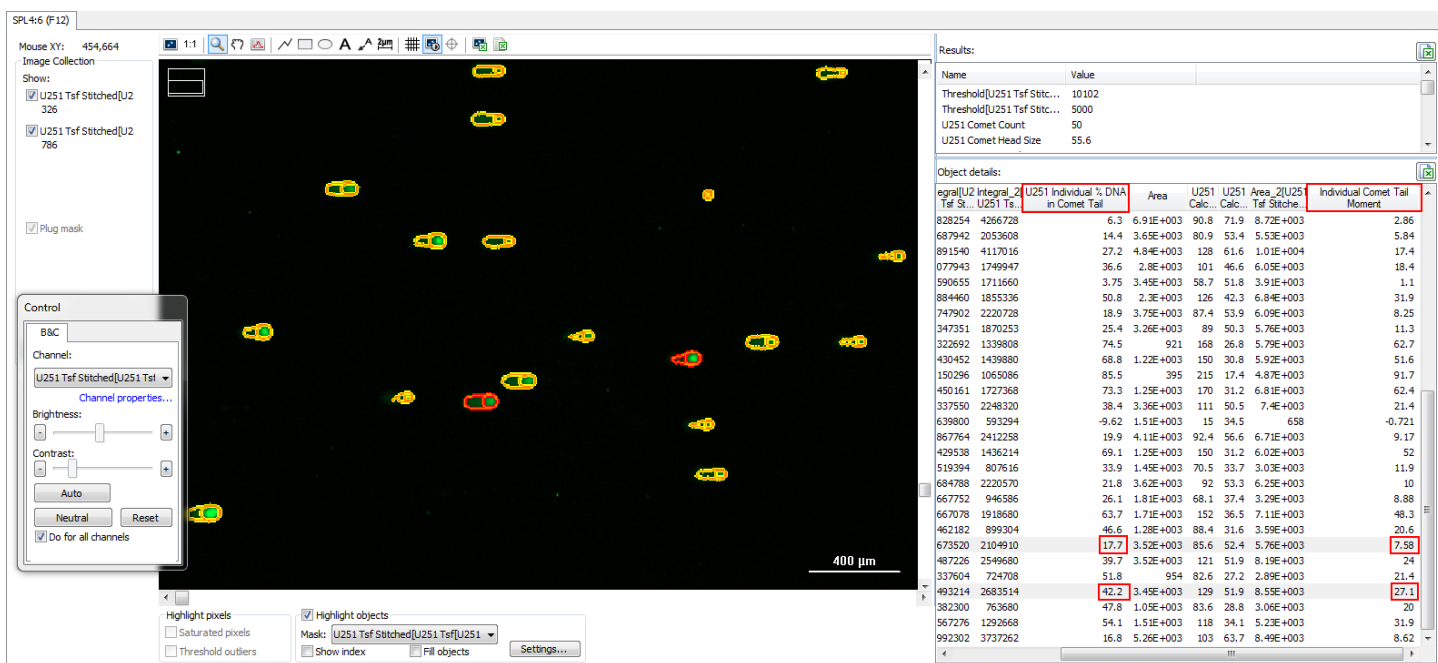


Figure 6. Screenshot of comet assay image demonstrating individual comet assay metric calculation.

Dual-mask comet assay validation data

Applying the formulas explained above, results for the comet population imaged from wells containing different camptothecin treatment levels were generated. As seen in Figure 7, both percent DNA in comet tail and tail moment values started low and increased appropriately as the concentration of camptothecin treatment increased, as was expected.

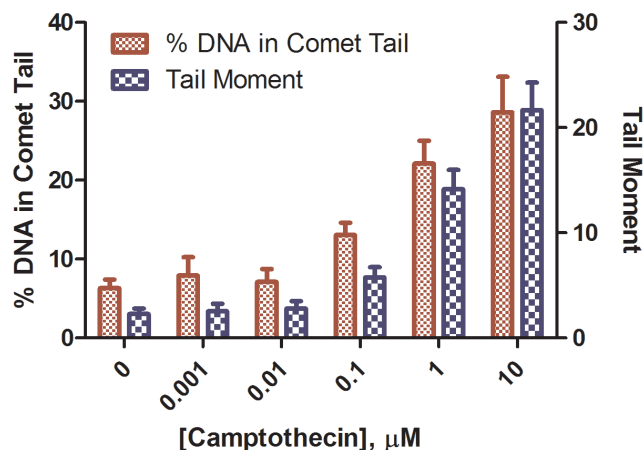


Figure 7. Percent DNA in comet tail and tail moment analyses using U251 cells exposed to various camptothecin concentrations. Four replicates tested at each compound concentration.

Data generated using the dual-mask analysis method was also compared to a previously validated method of comet assay analysis, which used a calculated metric based on the circularity of comets as DNA damage increases (Figure 8).

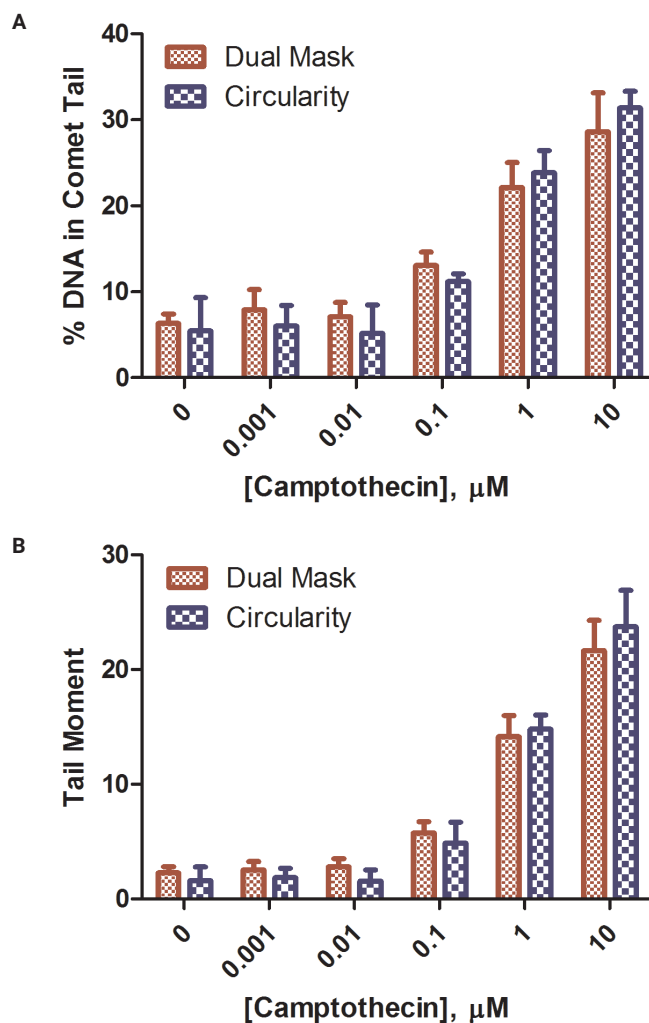


Figure 8. Comparison of generated (A) percent DNA in comet tail and (B) tail moment values using dual-mask or circularity analysis methods. U251 cells exposed to various concentrations of camptothecin. Four replicates tested at each compound concentration. Data from www.biotek.com/resources/articles/novel-comet-assay.html.

Results for both percent DNA in comet tail and tail moment agree across both methods, further validating the ability of the dual-mask method to deliver accurate, robust data on an individual comet and population basis. Using automated methods, both the percent DNA in the tail and comet tail moment calculations yielded consistent data across replicates, while reducing manual interpretations and sources of error, and saving time on manual calculations. The data may be compared to data from other analysis packages using circularity comet criteria.

Conclusion

Performing robust alkaline comet assays in a high throughput format reduces laboratory workflow bottle-necks compared to manual methods. Automated comet imaging through the Agilent BioTek Cytation 5 cell imaging multimode reader further enables high throughput efficiencies, with rapid imaging and a high degree of clarity to detect small changes in comet tail fluorescence. Dual masking enables population level analysis as well as single comet analysis, while common calculations, such as percent DNA in the tail and comet tail moment, are automatically and objectively determined in real time without requiring separate software, eliminating human subjectivity and error in the analysis that could potentially skew results. The combination of assay system along with automated imaging and analysis create a robust, user-friendly method when performing genotoxicity studies.

www.agilent.com/lifesciences/biotek

For Research Use Only. Not for use in diagnostic procedures.

RA44243.1301967593

This information is subject to change without notice.

© Agilent Technologies, Inc. 2016, 2021
Printed in the USA, December 14, 2021
5994-2595EN